© 2017. Published by The Company of Biologists Ltd | Journal of Experimental Biology (2017) 220, 3464-3477 doi:10.1242/jeb.162289

RESEARCH ARTICLE

Controlling thoracic pressures in cetaceans during a breath-hold dive: importance of the diaphragm

Margo A. Lillie[1,*], A. Wayne Vogl[2], Stephen Raverty[3], Martin Haulena[4], William A. McLellan[5], Garry B. Stenson[6] and Robert E. Shadwick[1]

ABSTRACT

Internal pressures change throughout a cetacean's body during swimming or diving, and uneven pressures between the thoracic and abdominal compartments can affect the cardiovascular system. Pressure differentials could arise from ventral compression on each fluke downstroke or by a faster equilibration of the abdominal compartment with changing ambient ocean pressures compared with the thoracic compartment. If significant pressure differentials do develop, we would expect the morphology of the diaphragm to adapt to its *in vivo* loading. Here, we tested the hypothesis that significant pressure differentials develop between the thoracic and abdominal cavities in diving cetaceans by examining diaphragms from several cetacean and pinniped species. We found that: (1) regions of cetacean diaphragms possess subserosal collagen fibres that would stabilize the diaphragm against craniocaudal stretch; (2) subserosal collagen covers 5–60% of the thoracic diaphragm surface, and area correlates strongly with published values for swimming speed of each cetacean species (P<0.001); and (3) pinnipeds, which do not locomote by vertical fluking, do not possess this subserosal collagen. These results strongly suggest that this collagen is associated with loads experienced during a dive, and they support the hypothesis that diving cetaceans experience periods during which abdominal pressures significantly exceed thoracic pressures. Our results are consistent with the generation of pressure differentials by fluking and by different compartmental equilibration rates. Pressure differentials during diving would affect venous and arterial perfusion and alter transmural pressures in abdominal arteries.

KEY WORDS: Cardiovascular, Collagen, Fluking, Diving mammal, Diving adaptations, Morphology

INTRODUCTION

Internal pressures change throughout a mammal's body during swimming or a breath-hold dive, and uneven changes between the thoracic and extra-thoracic compartments can produce pressure differentials that affect the respiratory and cardiovascular systems (Slijper, 1962). For arteries, what is commonly called blood pressure is more correctly a transmural blood pressure, calculated as the intra-arterial blood pressure minus the extra-arterial pressure exerted by surrounding tissue on the arterial wall (Fig. 1A). Intra-arterial pressure depends on thoracic pressure (plus the pressure generated by the heart on contraction), while extra-arterial pressure depends on the body region being perfused. Therefore, for consistent haemodynamics, thoracic pressure should be maintained relative to tissue pressures outside the thorax, or if this is not possible, the vascular system must be able to accommodate transient differences in regional pressures. In a study on the mechanical properties of fin whale arteries, we (Lillie et al., 2013) found most arteries lacked compliance and withstood sizeable negative pressures without collapse. We argued that such properties would be advantageous should arterial transmural pressures vary widely during a dive as a result of pressure differentials between the thorax and other regions of the body. In the current study, we examined the hypothesis that pressure differentials develop between the thoracic and abdominal cavities of diving cetaceans that put significant pressures on the diaphragm. We use 'diving' to include all underwater locomotion, including swimming near the surface. We identify here two possible ways a trans-diaphragmatic pressure differential, P_{di}, could develop. The first results from locomoting on a breath hold and the second from a transient effect of hydrostatic compression from ambient ocean pressures.

Fluking hypothesis

In most mammals, locomotion unavoidably deforms the rib cage, and the mechanical coupling between locomotion and respiration has been studied in terrestrial mammals (Bramble and Carrier, 1983; Perry and Carrier, 2006). Cetaceans generate thrust by oscillating their flukes vertically (Pabst, 1993). Spinal flexion should compress the ventral tissue on each downstroke (Lee and Banzett, 1997; Young et al., 1992), and therefore fluking on a breath hold could generate large thoracic pressure fluctuations (Fig. 1B) (Cotten et al., 2008). Cotten et al. (2008) argued that dolphins must be able to stabilize their thorax during locomotion to minimize thorax volume and pressure changes, and that this could include the diaphragm. Stabilizing the diaphragm limits expansion of the abdominal cavity into the thorax on each downstroke, diminishing pressure pulses within the thorax, but at the same time augmenting the pulses within the abdomen by preventing the release of abdominal pressure. That is, thoracic stabilization achieved by limiting the diaphragm's ability to deform comes at the cost of exacerbating any P_{di}. Pressure transients will last from under a second to a few seconds, depending on fluking frequency, and their magnitude should correlate with swim performance.

If the diaphragm is stabilized during fluking, then we predict there should be anatomical differences between the diaphragms of cetacea, which move their flukes vertically, and other marine mammals such as pinnipeds, whose aquatic locomotion is not based on vertical oscillation. Phocids, or true seals, produce thrust by

[1]Department of Zoology, University of British Columbia, Vancouver, BC, Canada V6T 1Z4. [2]Department of Cellular and Physiological Sciences, University of British Columbia, Vancouver, BC, Canada V6T 1Z3. [3]Animal Health Centre, 1767 Angus Campbell Road, Abbotsford, BC, Canada V3G 2M3. [4]Vancouver Aquarium Marine Science Centre, PO Box 3232, Vancouver, BC, Canada V6G 3E2. [5]Department of Biology and Marine Biology, University of North Carolina Wilmington, Wilmington, NC 28403, USA. [6]Fisheries and Oceans, Canada, St John's, NL, Canada A1C 5X1.

*Author for correspondence (lillie@zoology.ubc.ca)

M.A.L., 0000-0003-0763-0016

Received 4 May 2017; Accepted 17 July 2017

Journal of Experimental Biology

Journal of Experimental Biology (2017) 220, 3464-3477 doi:10.1242/jeb.162289

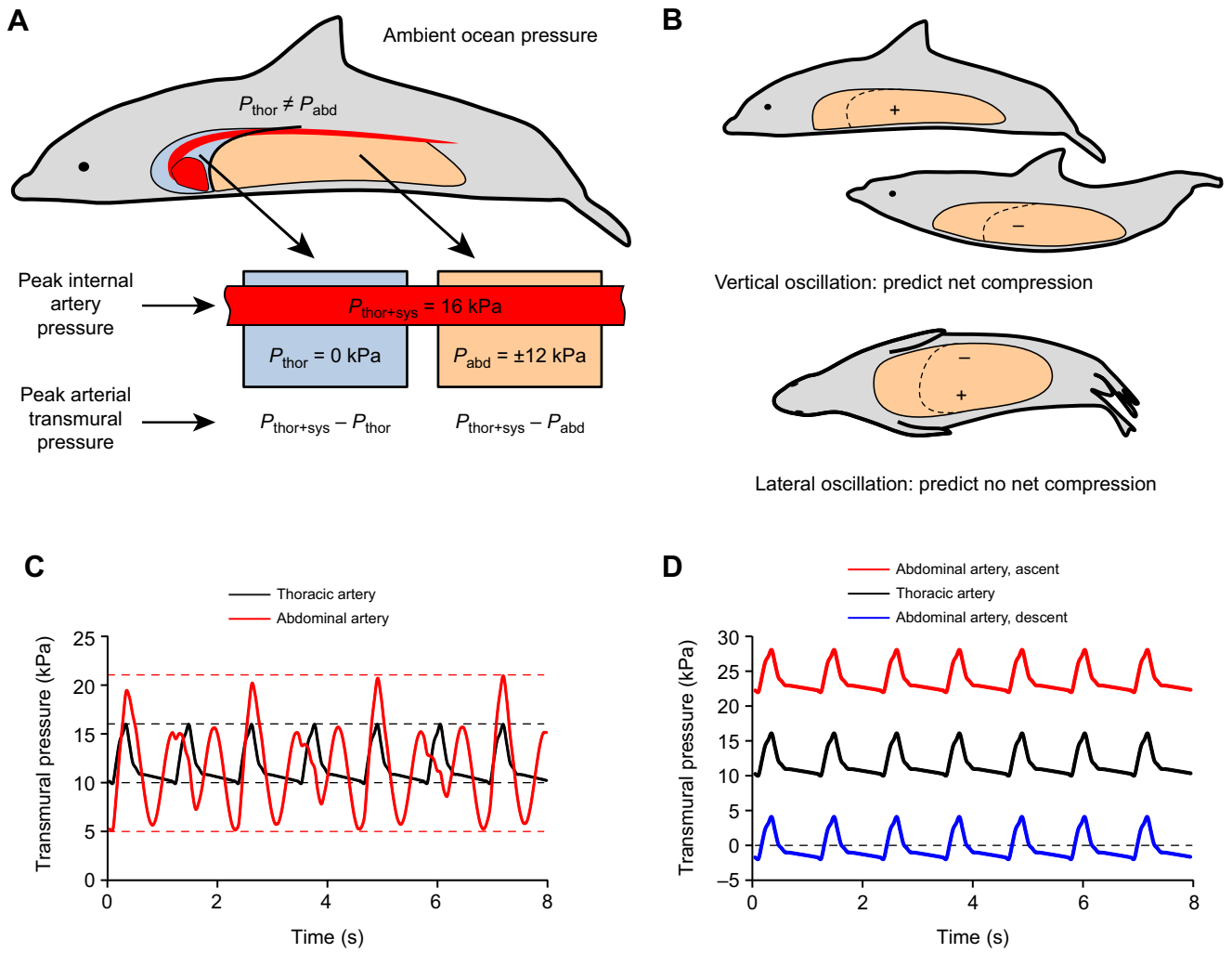

Fig. 1. Pressures within the body of a diving cetacean. (A) Thoracic (P_{thor}) and abdominal pressures (P_{abd}) may differ transiently during a dive, producing different arterial transmural pressures for arteries in the thorax and abdomen. Pressure values pertain to panel D. (B) In vertical oscillation, the bending axis lies above the thorax and abdomen. The tissue is alternately compressed and expanded, potentially producing a pressure pulse each downstroke. In lateral oscillation, the axis lies at the midline. One side of the body is compressed while the other expands, with no predicted net change in volume or pressure. (C) Arterial transmural pressures predicted by the fluking hypothesis for a thoracic and abdominal artery in an animal where fluking creates a ±5 kPa pressure pulse in the abdomen. The thoracic artery experiences only the cardiac pulse of 16/10 kPa. The abdominal artery experiences an expanded pressure range of 21/5 kPa as a result of constructive interference of cardiac and fluking waveforms. (D) Arterial transmural pressures predicted by the equilibration rate hypothesis for a thoracic and abdominal artery. On descent, abdominal pressures were set 12 kPa above thoracic pressures. Transmural pressures are normal in the thorax but drop in the abdomen because of the higher abdominal pressures. Predicted peak abdominal transmural pressure is low (16−12=4 kPa), and arteries face potential collapse. On ascent, abdominal pressures were set 12 kPa below thoracic pressures. Predicted peak abdominal transmural pressure is high (16+12=28 kPa), equivalent to hypertension.

lateral undulation of their hind flippers (Fish, 1996; Fish et al., 1988; Pierce et al., 2011), and, as has been postulated for running lizards (Carrier, 1987), lateral oscillations would expand one side of the thorax while compressing the other, with minimal net change in thoracic volume and hence thoracic pressure (Fig. 1B). Sea lions swim by oscillating their foreflippers (English, 1976; Feldkamp, 1987), which may generate little abdominal compression and only small changes of bilateral thoracic volume. Sea otters use a range of locomotory patterns, including stroking with hind legs and tail and vertical oscillation of the caudal half of the body (Kenyon, 1969; Tarasoff et al., 1972; Williams, 1989). It is unclear whether the thorax would be significantly compressed in these otters.

Equilibration rate hypothesis

Ambient ocean pressures change continuously while an animal changes depth, and transient pressure differences will arise between the thorax and abdomen if the two compartments equilibrate to ambient pressure at different rates. During a dive, ambient pressure acts directly on the body wall. For simplicity, we assume the abdominal body wall cannot support a significant pressure differential, and therefore abdominal pressure is the same as ambient pressure (Brown and Butler, 2000). In the thorax, air compression allows ambient pressure to compress the rib cage and the increased abdominal pressure to enhance venous influx into the thorax and to push the diaphragm dorsally and cranially. As the latter two shifts are driven by a positive abdomen-to-thorax pressure difference, the rise in thorax pressure most likely lags the rise in abdominal pressure during descent. Given ambient pressures increase at 20–30 kPa s^{-1} for descent rates of 2–3 m s^{-1}, even a small lag can lead to significant pressure differentials between the thorax and abdomen. Pressure transients will last from a few seconds to a few minutes, depending on descent (or ascent) rate and dive depth. Transients should disappear below alveolar collapse depth. The rate at which ambient pressures change

Journal of Experimental Biology (2017) 220, 3464-3477 doi:10.1242/jeb.162289

depends on descent rate, so the magnitude of any P_{di} may correlate with swim performance.

In the current study, we examined the morphology of diaphragms from several species of cetaceans and pinnipeds, looking for evidence of stabilization against a significant P_{di}. In particular, we looked at the amount and disposition of collagen fibres that would allow a diaphragm to withstand deformation. However, all diaphragms contain collagenous structures, and these serve different functions. In the absence of direct testing, establishing a stabilizing role of any observed collagen must be done through inference. Collagen typically has a J-shaped load–length curve: at short lengths, collagen fibres are slack and resist deformation weakly, but once the slack is taken up, the fibres are recruited and strongly resist further lengthening. Establishing the recruitment point is key to identifying when the fibres are loaded. A fibre cannot be recruited where diaphragm stretch is prevented by a supporting structure on the thoracic side. For example, in the 'zone of apposition' where the diaphragm is in contact with and supported by the ribs, any pressure differential will develop across the ribs, not the diaphragm, and the P_{di} across the diaphragm itself will be minimal (Angelillo et al., 2000; Loring and Mead, 1982; Urmey et al., 1988).

We predicted the following for a diaphragm stabilized against deformation under a P_{di}. (1) Collagen will be deposited on the diaphragm in response to elevated loads. Loads depend directly on the P_{di}, but also on local diaphragm curvature, gravity and any local support provided by surrounding structures. Therefore the distribution, orientation and quantity of collagen on the diaphragm of a diving mammal should reflect the local need to resist or allow passive lengthening. The distribution will be consistent with loading associated with diving and not consistent with loading associated with respiration. (2) As both hypotheses link the generation of P_{di} to locomotion, recruitment must be possible over a range of depths and diaphragm muscle lengths, without hindering any diaphragm lengthening necessary for lung compression. This can be achieved by connecting collagen 'in series' with muscle fibres (i.e. end-to-end), as opposed to 'in parallel' (side-by-side). (3) Once the alveoli collapse, the lungs become essentially incompressible (Fitz-Clarke, 2007), and therefore protection from abdominal loads is not needed below the depth of alveolar collapse. If these three predictions hold, we can conclude that cetaceans experience significant P_{di}. In addition, the fluking hypothesis predicts: (4) more collagen on cetacean diaphragms compared with those of pinniped, and (5) the amount of collagen will correlate with some measure of swim performance. The equilibration rate hypothesis does not specifically predict whether the diaphragm would facilitate or resist deformation, so the presence of ample collagen per se (prediction 1) is inconclusive. It also makes no specific predictions about pinnipeds (prediction 4), but is compatible with prediction 5. We found structural differences between cetacean and pinniped diaphragms compatible with both fluking and equilibration rate hypotheses. Our results indicate cetaceans and pinnipeds experience different internal pressures during a dive.

MATERIALS AND METHODS

Details of the animals used in this study are listed in Table 1. A total of 42 diaphragms were obtained from several sources. The majority of diaphragms were collected at necropsy of animals stranded and recovered along the coast of British Columbia, Canada, by the Marine Mammal Rescue Program or the Marine Mammal Rescue Centre, Vancouver Aquarium, Canada. Additional specimens were obtained from the Vancouver Aquarium. A minke whale diaphragm was obtained from a stranded animal collected by the Marine Mammal Stranding Program at the University of North Carolina Wilmington, USA, under NOAA stranding permits. Harp seal diaphragms were collected as part of a biological sampling programme undertaken by Fisheries and Oceans, Canada in Newfoundland. Seals were collected according to the Fisheries Act. Fin whale diaphragms were collected from fresh fin whale carcasses as part of a commercial whaling operation at Hvalfjörður, Iceland, during the summers of 2013 to 2015. Material obtained outside Canada was imported under the Convention on International Trade in Endangered Species of Wild Fauna and Flora (CITES) permits. Pig and sheep diaphragms were obtained fresh after slaughter for other purposes from local farmers.

When possible, diaphragms were harvested intact by incising the distal diaphysis of the ribs parallel to the coastal arch, transverse

Table 1. List of animals studied

Order (suborder)	Family	Species and taxonomic authority	Common name	Age class, no. and sex
Carnivora (Pinnipedia)	Phocidae	*Mirounga angustirostris* (Gill)	Northern elephant seal	Juvenile 1M
Carnivora (Pinnipedia)	Phocidae	*Phoca vitulina* Linnaeus	Harbour seal	Adult 1M
Carnivora (Pinnipedia)	Phocidae	*Pagophilus groenlandicus* Erxleben	Harp seal	Adult 1M 2F
Carnivora (Pinnipedia)	Otariidae	*Eumetopias jubatus* Schreber	Steller sea lion	Sub-adult 1M
Carnivora (Pinnipedia)	Otariidae	*Zalophus californianus* (Lesson)	California sea lion	Adult 1M
Carnivora	Mustelidae	*Enhydra lutris* (Linnaeus)	Sea otter	Sub-adult 1M Adult 3M
Cetartiodactyla (Odontoceti)	Phocoenidae	*Phocoena phocoena* (Linnaeus)	Harbour porpoise	Fetus 1M Calf 1M 1F Sub-adult 1M 3F Adult 1M 3F
Cetartiodactyla (Odontoceti)	Phocoenidae	*Phocoenoides dalli* (True)	Dall's porpoise	Sub-adult 1M Adult 1M 1NA
Cetartiodactyla (Odontoceti)	Delphinidae	*Lagenorhynchus obliquidens* (Gill)	Pacific white-sided dolphin	Adult 1M 2F
Cetartiodactyla (Odontoceti)	Delphinidae	*Orcinus orca* (Linnaeus)	Killer whale	Calf 1F
Cetartiodactyla (Odontoceti)	Monodontidae	*Delphinapterus leucas* (Pallas)	Beluga whale	Adult 1F
Cetartiodactyla (Mysticeti)	Balaenopteridae	*Balaenoptera physalus* (Linnaeus)	Fin whale	Fetus 1M 1F Adult 2M 1F
Cetartiodactyla (Mysticeti)	Balaenopteridae	*Balaenoptera acutorostrata* Lacépède	Minke whale	Calf 1M
Cetartiodactyla	Suidae	*Sus scrofa* Linnaeus	Pig	Sub-adult 2M
Cetartiodactyla	Bovidae	*Ovis aries* Linnaeus	Sheep	Juvenile 1NA Sub-adult 3NA

M, male; F, female; NA, sex not available.

Journal of Experimental Biology (2017) 220, 3464-3477 doi:10.1242/jeb.162289

removal of the sternibrae and dissection of 1–2 thoracolumbar vertebrae. The pericardium, pericardial venous plexus, mesoesophagus and associated connective tissues were removed, and, except where noted, the parietal pleura and peritoneum were left intact. The oesophagus and posterior vena cava were frequently removed at necropsy. Diaphragms were in excellent to moderate post-mortem condition and were examined fresh where possible or frozen at the time of necropsy for later evaluation. Overall diaphragm morphology was examined using gross dissection. Diaphragms that did not lie flat were draped over a flexible plastic support for study. For smaller species, muscle and collagen fibre orientation was verified under a dissecting microscope.

The fraction of the thoracic surface covered by collagen not associated with the pleura was determined from photographs using ImageJ. For specimens that did not lie flat, combined areas were calculated from dorsal, cranial and lateral views. As tissue was sometimes missing from the edges of the specimen, the reported values probably overestimate the true area, but there should be no bias according to species. Values for cruising and maximum swimming speeds in m s^{-1} were taken from Fish and Rohr (1999) and Lang and Daybell (1963) and converted to body lengths (BL) s^{-1} using data from Blix and Folkow (1995), Fish and Rohr (1999), Lockyer and Waters (1986) and Williamson (1972). We used a linear regression model to assess the relationship between mean collagen area fraction and species cruising and maximum swimming speeds.

Samples used for histological study were taken only from fresh (unfrozen) diaphragms. Samples were collected from costal and crural muscle from areas showing minimal collagen fibres on the surface and fixed in 10% phosphate-buffered formalin. After embedding, paraffin sections were cut at 5 µm and stained with Verhoeff's Van Gieson, which stains collagen dark red, muscle pink and elastin black.

RESULTS

Terrestrial mammal diaphragm

The basic structure of a terrestrial mammal diaphragm is shown by the pig diaphragm in Fig. 2A. The diaphragm is composed of costal and crural muscles joined by the horns of a collagenous central tendon. Collagen surrounds the vena cava at the apex of the central tendon. Thoracic and abdominal surfaces are covered with visceral and parietal pleural and peritoneal serosal membranes, respectively, with associated fascia (left side of Fig. 2A). In the pig and sheep, the fascia was thick in both the pleura and peritoneum, adhering firmly to the central tendon but weakly to underlying muscle. No other collagen was visible on the surface. Intramuscular collagen was present in all diaphragms studied (terrestrial and diving mammals), but we do not report on it.

Diving mammal diaphragm

Diaphragm collagen in sea otters and pinnipeds is shown in Figs 2B and 4, respectively. Diaphragm collagen in cetaceans is summarized in Fig. 3 and shown in Figs 5–7. Images are generally oriented dorsal up.

Diving mammal central tendon

Diving mammals lacked the broad central tendon of the two terrestrial mammals. Instead of the horns of the central tendon, costal and crural muscles were joined by a much reduced collagen-rich seam, termed here the costo-crural junction, CCJ. This is clearly visible in the sea otter in Fig. 2B and the pinnipeds in Fig. 4A,C,D,F, G and less visible in the cetaceans in Figs 5A,C,G and 6D,G. The junction was thinner at the caudal end and broadened cranially, with generally more collagen on the right side than the left, such that in many individuals the CCJ on the right side broadened into a complex tendinous aponeurosis. This is illustrated in a harp seal (Fig. 4H), where the orthogonal collagen fibres reflect the orientation of the costal and crural muscle that insert directly onto it, and in a fin whale (Fig. 6G).

In non-cetacean diving mammals, the medial part of the central tendon was also much reduced so that the caval hiatus was surrounded by a mix of muscle and collagen (Figs 2B and 4A–D,F). This collagen was continuous with the CCJ. The caval hiatus of the harp and harbour seals was encircled by a substantial ring of collagen, particularly visible from the abdominal side (Fig. 4B), separating the caval sphincter muscle from the diaphragm. All non-cetacean diving mammals showed more collagen to the left of the caval hiatus than to the right. In the sea otter and California sea lion,

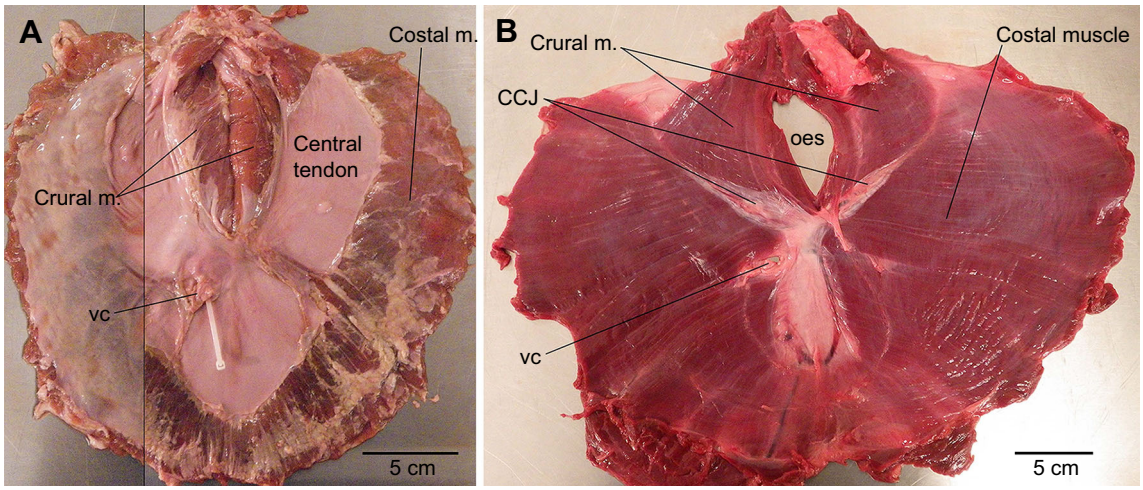

Fig. 2. Thoracic surface of the diaphragm from a terrestrial mammal and a non-cetacean diving mammal. (A) Pig. Costal and crural diaphragm muscles are joined by the horns of the central tendon. Tissue at the left of the image remains covered by the pleura. On the right, the pleura overlying the costal muscle was removed, but remained tightly adhered to the central tendon. The oesophagus was removed, and the oesophageal hiatus lies between two arms of crural muscle. A plastic strap marks the caval hiatus. (B) Sea otter. The horns of the central tendon are reduced to a collagenous costo-crural junction (CCJ). A medial aponeurosis lies to the left of the caval hiatus. The oesophagus was removed. vc, vena cava or caval hiatus; oes, oesophagus or oesophageal hiatus.

Journal of Experimental Biology (2017) 220, 3464-3477 doi:10.1242/jeb.162289

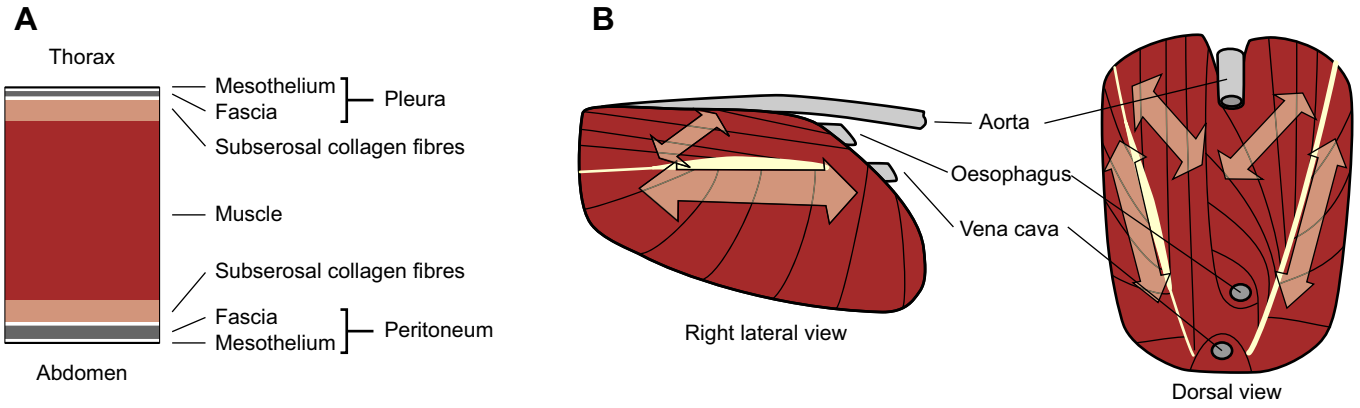

Fig. 3. Summary diagrams of muscle and collagen morphology of cetacean diaphragms. (A) Cross-section through the diaphragm, showing layering of structures through the region with subserosal collagen on both the thoracic and abdominal sides. (B) Two views of the thoracic surface. Black lines show the orientation of muscle fibres. White indicates collagen of the CCJ. Arrows show the general location and orientation of subserosal collagen.

this left collagen broadened into a large aponeurosis visible from both thoracic and abdominal sides (Figs 2B and 4C). The cetacean caval hiatus was encircled by a complex mix of muscle and collagen, but we observed no major collagenous structure encircling the hiatus or constraining the caval opening (Figs 5E and 6G).

Diving mammal subserosal collagen

Some of the muscle on the cetacean diaphragms was overlain with collagen fibres running under the fascia of the pleura and peritoneum (Fig. 3A). We refer to this as 'subserosal collagen'. Such subserosal collagen was not observed in non-cetacean diaphragms. The density of these collagen fibres varied regionally, although there was much inter- and intra-species variation. On the thoracic surface, there were two dominant concentrations, one coursing roughly craniocaudally over the costal muscle and one coursing laterocaudally over the crural muscle (Fig. 3B). Much of the subserosal collagen on the costal muscle followed the orientation of the crural muscle on the other side of the CCJ (Fig. 5C,E,G), and the subserosal collagen on the crural muscle followed the orientation of the costal muscle across the CCJ (Figs 5G and 6C) or of the crural muscle across the midline (Fig. 5B). Over the crural muscle on the thoracic side, collagen density was higher caudally (Figs 5B,F,G and 6A), whereas, more anteriorly, the subserosal collagen was largely absent over a large region dorsocaudal to the oesophageal hiatus (Figs 5A,E and 6A,D). Over the costal muscle on the thoracic side, collagen density was highest near the CCJ and decreased ventrally, becoming negligible within the zone of apposition between the muscle and ribs, close to the diaphragm insertion on the chest wall (Figs 5C,G and 6C,E). Throughout the cranial aspect of the diaphragm, subserosal collagen was structurally complex and sometimes displayed no predominant orientation. On the abdominal side, subserosal collagen fibres formed two arrays of parallel fibres (Fig. 7). This is the most consistent collagen feature observed, and it was present to varying extents in every cetacean diaphragm examined, including neonates and late term fetuses. Ventrally, the arrays started lateral to the vena cava and ran dorsocaudally. Abdominal subserosal collagen was sometimes dense dorsal to the vena cava, especially towards the right (Fig. 7A), and in some animals the pattern of subserosal collagen seen over the crural diaphragm on the thoracic side was repeated on the abdominal (Fig. 7E).

In-series connections between one end of a subserosal collagen fibre and individual muscle fibres were clearly present on both the thoracic and abdominal surfaces: on the abdominal side at the ventral ends of the parallel array (Fig. 7A–D) and on the thoracic side at the dorsal midline (Fig. 5B) and at the CCJ (Figs 5C and 6C). Subserosal collagen fibres terminated at the other end by merging into the CCJ or into the pleural fascia, by inserting again onto a muscle fibre (Fig. 7B), or by interconnecting with other collagen fibres (Fig. 5B).

The amount of subserosal collagen varied with species, and younger animals may possess less subserosal collagen than older ones. Fig. 8A shows the fraction of the thoracic surface covered with subserosal collagen or collagen associated with the CCJ. Only 5% of the minke and beluga whale diaphragms were covered with collagen, while 60% of the Dall's porpoise diaphragm was covered. Little subserosal collagen was visible in the fin whale, possibly because it was difficult distinguishing between it and the particularly thick pleural fascia. Although the amount of collagen on cetacean diaphragms varied with species, as a group there was clearly more collagen on the cetacean diaphragms than on the diaphragms of non-cetacean diving mammals (Fig. 8A). If collagen is deposited on cetacean diaphragms in response to loads generated by locomotion, then collagen content should correlate with some measure of swim performance. The percentage of total surface area covered by collagen correlated with cruising (P<0.001) and maximum swim speed (P=0.002; Fig. 8B).

Diving mammal pleural and peritoneal fascia

Thoracic and abdominal surfaces were invested by visceral and parietal pleural and peritoneal serosa with associated serosal fascia (Fig. 3A). In each animal, the pleural and peritoneal fascia could be removed easily from some areas (Fig. 9A) but adhered to others (Fig. 9B). Diaphragm surface area increased after the fascia was removed, indicating the fascia was under tension and the muscle under compression in the unloaded diaphragm.

Pleura and peritoneum were examined histologically in three non-cetacean diving marine mammals and three cetaceans. Pleural and peritoneal composition was similar in all species, containing mostly collagen with relatively little elastin (Fig. 9E) and varying amounts of adipose tissue. Collagen fibre density and organization varied (Fig. 9C–E). In all species, fascial collagen ran perpendicular to the underlying muscle (Fig. 9A–E). Fascial thickness varied from 0.1 mm in the sea otter to 3.1 mm in the fin whale. The peritoneum tended to be thicker than the pleura, being 20–50% thicker in pinnipeds and sea otters and up to 200% in cetaceans. The combined pleural plus peritoneal thickness accounted for ∼5% of the total diaphragm thickness in sea otters and beluga, and ∼15% in

Journal of Experimental Biology (2017) 220, 3464-3477 doi:10.1242/jeb.162289

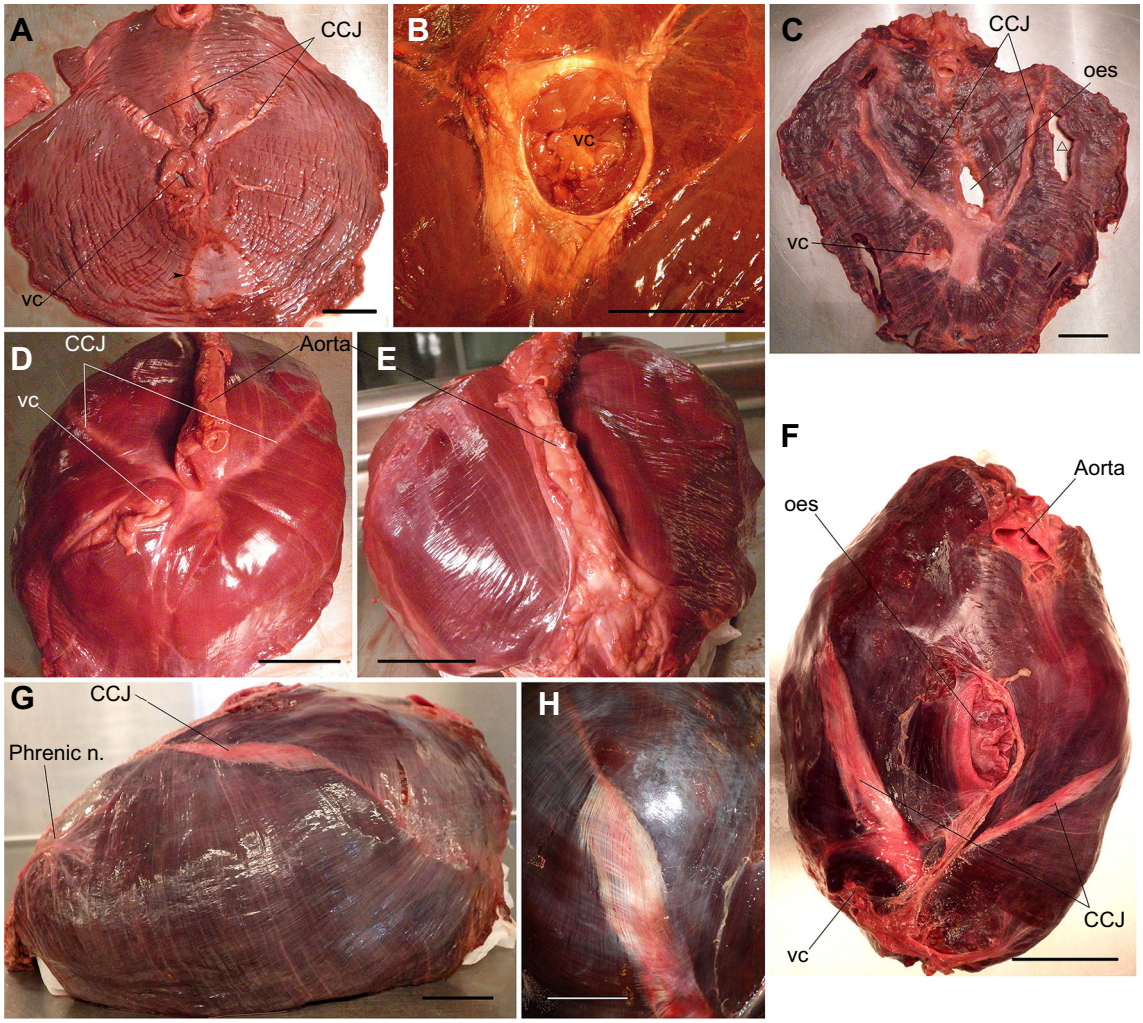

Fig. 4. Morphology of pinniped diaphragms. (A,B) Harbour seal. (A) Thoracic side. Most of the pericardium was removed, although some remained (arrowhead). The oesophagus was removed. The ring of muscle around the caval opening is the remnant of the caval sphincter. (B) Collagen ring around the caval hiatus, viewed from the abdominal side. The thicker band on the left is visible on the thoracic side in A and is continuous with the left CCJ. (C) California sea lion. Thoracic side, showing the much reduced central tendon horns and an aponeurosis to the left of the caval hiatus. The triangle indicates tissue damaged during necropsy. (D,E) Steller sea lion. Dorsocranial and posterior views. The crura were broad. A caval sphincter is visible as a loop of muscle arching over the caval hiatus. To the left of it was a collagenous tendon connecting to the CCJ. (F–H) Harp seal. Dorsal (F) and left lateral (G) views, showing the CCJ and muscle covered with the pleura (G) but no other collagen. (H) Close-up of the right CCJ showing two orientations of collagen fibres. Scale bars, 5 cm.

California sea lion and Pacific white-sided dolphin (Fig. 9F). For comparison, thickness averaged 11% in the sheep, matching other terrestrial diaphragms (Boriek and Rodarte, 1994; Chamberlain et al., 2007; Griffiths and Berger, 1996; Griffiths et al., 1992). We found no difference in total fascial thickness between cetaceans and non-cetaceans. Although these values are based on few measurements, these results suggest the serosal fascia is consistent in diving marine and terrestrial mammals.

DISCUSSION

This study tested the hypothesis that pressure differentials between the thoracic and abdominal cavities exist in diving cetaceans and significantly load their diaphragms. As variation in diaphragm morphology reflects differences in *in vivo* loading, we examined the morphology of diaphragms of different diving marine and non-diving terrestrial mammals to identify features related to the internal biomechanical environment during a dive. Resisting significant loading would require the deposition of collagen to stiffen the diaphragm. We found differences in the amount and organization of diaphragmatic collagen between diving and non-diving mammals, between the groups of diving mammals, and within the cetaceans as a group. Here, we first consider the likely mechanical role of each form of diaphragmatic collagen, and we argue the results are consistent with the hypothesis that cetacean diaphragms are loaded under a significant P_{di} during a dive. In the second part of the Discussion, we consider the fluking and equilibration rate hypotheses as potential sources of P_{di}. Finally, we consider the possible impact of P_{di} on arterial pressures.

We found collagen associated with four structures of the mammalian diaphragm: (1) central tendon, (2) collagen of the pleural and peritoneal fascia, (3) regional subserosal collagen fibres between the fascia and muscle surface, and (4) intramuscular collagen. We do not discuss intramuscular collagen. Although we treat subserosal collagen here as categorically separate from serosal fascia, the two groups may represent different points along a continuum in which collagen fibre density, orientation and connections to muscle are principal parameters that vary in degree. The distribution of the first three forms of collagen

Journal of Experimental Biology

Journal of Experimental Biology (2017) 220, 3464-3477 doi:10.1242/jeb.162289

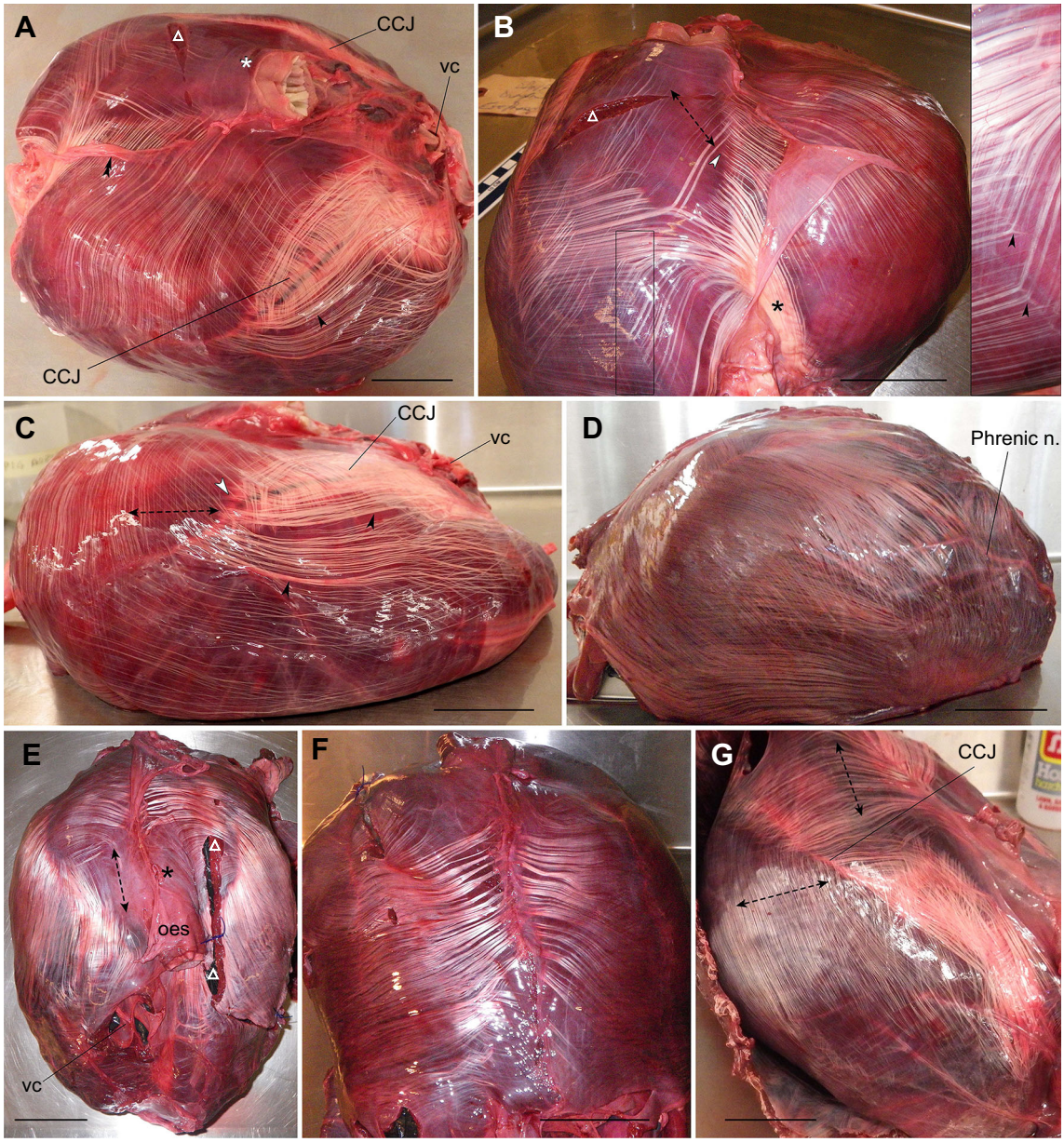

Fig. 5. Thoracic surface of cetacean diaphragms showing ample subserosal collagen. (A–C) Pacific white-sided dolphin. (A) Dorsal view showing collagen over the broad crural diaphragm between the right and left CCJ. Collagen is absent just caudal to oesophageal hiatus (asterisk). Much subserosal collagen overlies the CCJ and nearby costal muscle (arrowhead). No comparable structure exists on the left. A small amount of pleura at the midline has been peeled back (double arrowhead). (B) Posterior view showing the asymmetry of the subserosal collagen. Subserosal collagen fibres connect in series with crural muscle fibres (white arrowhead). Inset shows a close-up of the boxed area showing the splitting of collagen fibres around muscle fibres (arrowheads). (C) Right lateral view. Large subserosal collagen fibres connect in series with crural muscle fibres (white arrowhead) and overlie the costal muscle particularly just below the CCJ (arrowheads). Finer collagen fibres overlie the costal and crural muscle. (D–F) Dall's porpoise. (D) Right lateral view. Dense subserosal collagen largely obscures underlying muscle. (E) Dorsal view showing the collagen-free area just caudal to the oesophageal hiatus (asterisk). (F) Posterior view showing symmetrical subserosal collagen over the crura. Note the layering of collagen and muscle fibres near the midline. (G) Harbour porpoise. Right lateral view of the diaphragm held with the caudal end elevated. Subserosal collagen orientation on one side of the CCJ matches the underlying muscle orientation on the other side of the CCJ. Scale bars, 5 cm. The triangles in A, B and E indicate tissue damaged during necropsy. Double-headed arrows show muscle orientation.

showed consistent patterns in the seven cetacean species studied. Cetacean fascial collagen appeared functionally similar to that of terrestrial diaphragms; however, the reduction of the central tendon and the deposition of ample subserosal collagen on cetacean diaphragms differ from our findings in terrestrial mammals.

Central tendon is much reduced in diving mammals

As previously reported, the first notable difference between diving and terrestrial mammal diaphragms was the severe reduction of the central tendon (Le Double, 1897; Slijper, 1962). This may constitute a general diving adaptation. Reducing the central tendon in a diving mammal has clear benefits: longer muscles have greater shortening potential; reduction may facilitate diaphragm shape change at depth (Boriek and Rodarte, 1997); and muscle around the caval hiatus, instead of pure collagen, may alter flow, comparable to the caval sphincter in pinnipeds (Barnett et al., 1958; Harrison et al., 1954; Harrison and Tomlinson, 1956; Ronald et al., 1977).

Journal of Experimental Biology (2017) 220, 3464-3477 doi:10.1242/jeb.162289

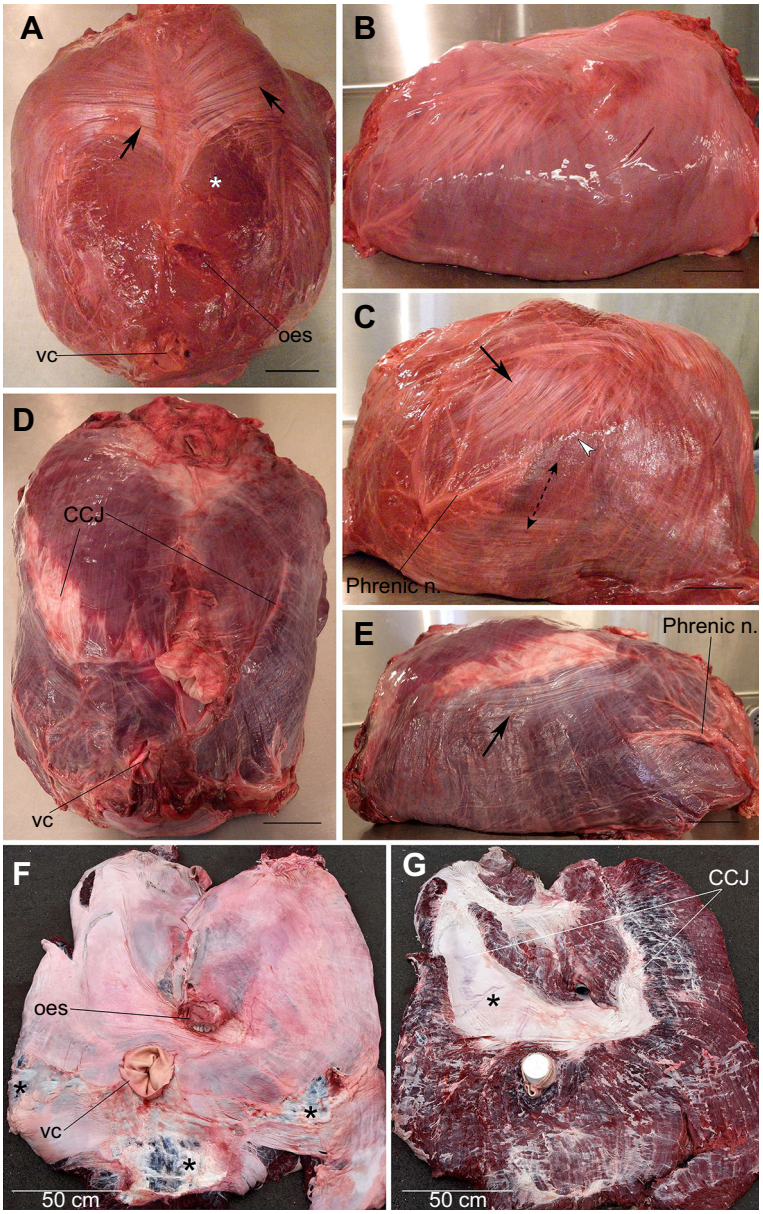

Fig. 6. Thoracic surface of cetacean diaphragms showing little to moderate subserosal collagen. (A–C) Killer whale calf. (A) Dorsal view. The pleura was largely removed. Subserosal collagen fibres (arrows) run symmetrically from the midline, laterocaudally across the crural muscle. Collagen is absent just dorsal to the oesophageal hiatus (asterisk). (B,C) Left lateral view before (B) and after removal of the pleura (C). Subserosal collagen fibres are visible in C (arrow), and some connect in series with costal muscle fibres (white arrowhead). (D,E) Minke whale. Dorsal and right lateral views showing dense collagen at the CCJ but minimal subserosal collagen elsewhere (arrow in E). (F,G) Fin whale. (F) The pleura covers the surface except where the phrenic nerves and pericardium have been removed (asterisks). (G) The pleura was removed. The CCJ is large on the right side (asterisk). Plastic has been inserted into the oesophageal and caval hiatuses. Scale bars, 5 cm (except where indicated). Double-headed arrows show muscle orientation.

Pleural and peritoneal fascia are similar in diving and non-diving mammals

All diving mammal diaphragms examined were covered with serosal fascia of the pleura and peritoneum that appeared structurally and functionally similar to those of terrestrial mammals. Fascial composition and relative thickness in diving mammals were similar to those of terrestrial mammals (Michailova and Usunoff, 2006; and Fig. 9F). Additionally, the observed morphological bias towards muscle cross-fibre orientation in diving mammals agrees with the higher cross-fibre stiffness measured in isolated fascia (Strumpf et al., 1989) and in intact diaphragm muscle (Boriek et al., 2000, 2001; Gates et al., 1980; Hwang et al., 2005; Strumpf et al., 1993). Fascial collagen fibres were connected largely in parallel with underlying muscle, as opposed to in series. Although some load transfer between the fascia and muscle would be possible in regions of high fascial adhesion (Fig. 9B), the same would occur in terrestrial diaphragms.

In terrestrial mammals, the fascia resists deformation at long muscle lengths (Gosselin et al., 1994; Griffiths and Berger, 1996; Griffiths et al., 1992; Kim et al., 1976; Mardini and Mccarter, 1987; McCully and Faulkner, 1983; Road et al., 1986), which, at least in dogs, occurs at the lowest lung volumes (De Troyer and Wilson, 2009; Farkas and Rochester, 1988; Kim et al., 1976; Margulies et al., 1990; Road et al., 1986). If cetacean facia has the same function, it must be recruited close to alveolar collapse. These results indicate collagen associated with fascia in cetaceans cannot stabilize the diaphragm against dive-associated P_{di}: the fascia cannot operate over a range of depths because it runs in parallel with muscle (contrary to prediction 2); it is probably recruited at alveolar collapse (contrary to prediction 3); and no quantitative differences between cetaceans and pinnipeds were observed (Fig. 9F, contrary to prediction 4). We have found no diving adaptations in the fascia of the marine mammals examined.

Subserosal collagen fibres stabilize cetacean diaphragms relative to swim speed

The second notable feature of cetacean diaphragm collagen was the presence of sometimes large collagen fibres on the diaphragm

Journal of Experimental Biology (2017) 220, 3464-3477 doi:10.1242/jeb.162289

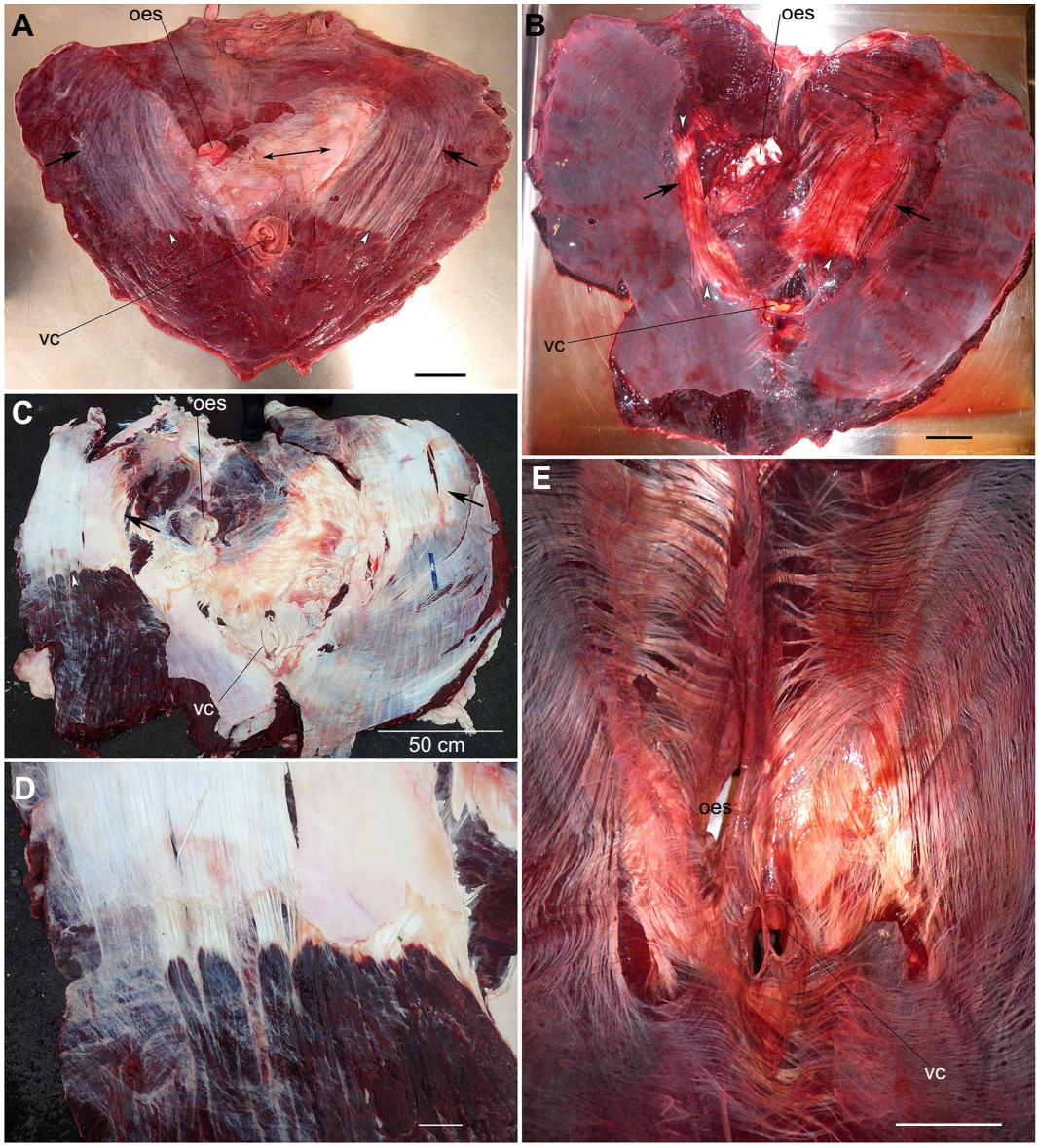

Fig. 7. Abdominal surface of cetacean diaphragms showing subserosal collagen. (A–C) Two arrays of parallel subserosal collagen fibres (arrows) start near the vena cava and run caudally. This collagen connects in series with muscle fibres (white arrowheads). (A) Minke whale. The peritoneum has been removed. A dense patch of thick collagen fibres crosses the midline, with orientation shown by the double arrow. (B) Beluga whale. The peritoneum was removed from the crural diaphragm but remains over most of the costal muscle. (C) Fin whale. The peritoneum was removed from most of the left side but remains on the right. (D) Detail of C. (E) Dall's porpoise. The peritoneum was removed. Much subserosal collagen overlies the costal and crural muscle with the same pattern as seen on the thoracic side in Fig. 5F,G. Scale bars, 5 cm (except where indicated).

surface under the serosal fascia. We know of no previous reports of this collagen. Subserosal collagen fibres were absent on terrestrial, pinniped and sea otter diaphragms, and so the feature represents a difference not between terrestrial and diving mammals but between the three groups of diving mammals.

On the cetacean diaphragm, regional distribution, orientation and quantity of subserosal collagen were consistent with the local need to resist or allow passive lengthening. Subserosal collagen was absent immediately caudal to the oesophageal hiatus where local stretch of the crural diaphragm is necessary to accommodate swallowing, and it was also largely absent from the more ventral parts of the costal muscle, in the zone of apposition where loads would be supported by adjacent ribs. On the thoracic side, sometimes substantial amounts of subserosal collagen overlay the crural muscle somewhat caudal to the oesophageal hiatus, and it overlay the costal muscle, especially near the CCJ (Fig. 3). On the abdominal side, an array of parallel collagen fibres starting near the level of the vena cava was consistently present (Fig. 7). The amount of subserosal collagen varied among species, but its orientation was consistent to hinder craniocaudal stretch of the costal diaphragm and laterocaudal stretch of the caudal crural diaphragm (Figs 3, 5 and 6), consistent with loading by a P_{di} during a dive.

Although many subserosal collagen fibres could not be traced to their ends, a large number were connected in series to a muscle fibre at one end and often terminated diffusely into the serosal fascia at the other. This is an important difference from the serosal fascia, which was connected in parallel with muscle. In-series collagen-to-muscle connections were clearly present on the abdominal side at the ventral end of the parallel array (Fig. 7), and on the thoracic side

Journal of Experimental Biology (2017) 220, 3464-3477 doi:10.1242/jeb.162289

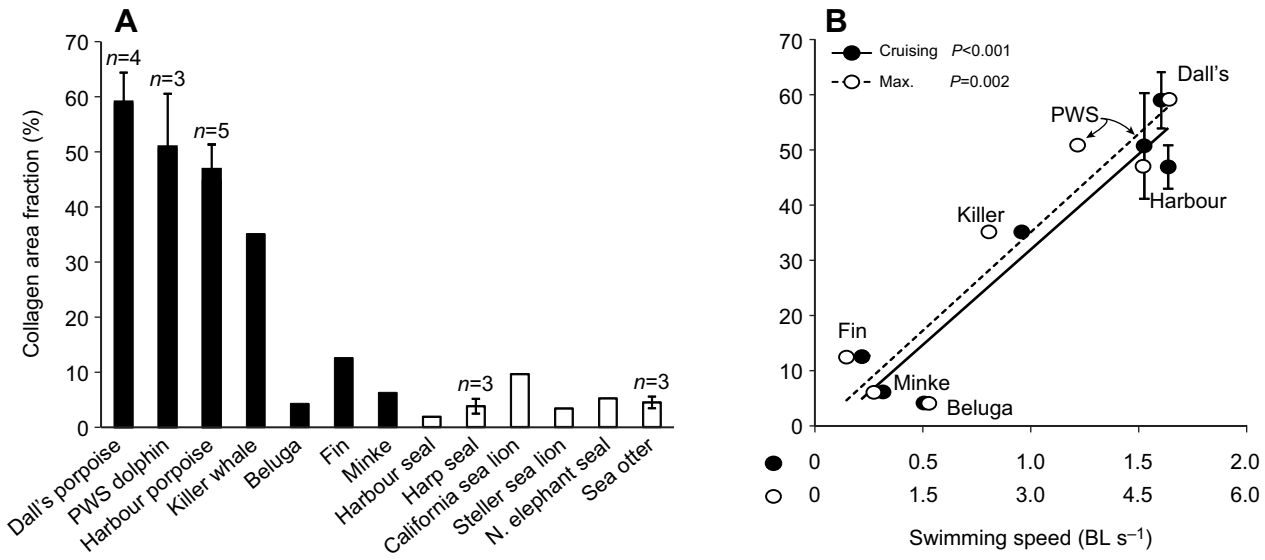

Fig. 8. Thoracic collagen content. Collagen area fraction is the area covered by thoracic subserosal collagen and collagen associated with the CCJ relative to the total area. (A) Collagen area varied in cetaceans but was minimal in pinnipeds and sea otters. (B) Collagen area in cetaceans correlated significantly with cruising and maximum swim speeds expressed as body lengths (BL) s^{-1} (linear regression). Where data are from more than one animal, values are given as means±s.e.m.

at the dorsal midline (Fig. 5B) and at the CCJ (Figs 5C and 6C). Although all muscle fibres connect in series to collagen at the CCJ, the subserosal collagen fibres of interest here crossed the CCJ and continued on the other side. Activation of one muscle (costal or crural) would recruit its associated subserosal collagen to carry loads over the other muscle without directly loading it. This arrangement would afford some measure of active control over diaphragm deformation in response to a P_{di}.

It is unlikely that the subserosal collagen is recruited during respiration, even the very short and forceful ventilatory cycles exhibited by some cetaceans (Piscitelli et al., 2013). Recruiting the subserosal collagen during expiration would inhibit diaphragm expansion necessary for volume reduction and so would be counterproductive. Recruitment at end expiration would be unnecessary if the serosal fascia bears the load at that stage, as proposed. During inspiration, one study showed the dog's diaphragm stretched most at its insertion at the chest wall as a result of rib cage expansion (Péan et al., 1991). If subserosal collagen in cetaceans is laid down in response to this inspiratory load, it should be densest at the insertion. However, we found minimal subserosal collagen along the whole ventral border where the diaphragm lies in apposition to the ribs (Figs 5 and 6). The deposition of subserosal collagen does not appear to be driven by forces associated with either inspiration or expiration (prediction 1). If the subserosal collagen is not loaded during respiration at the surface, then it is loaded at some point during a dive.

Subserosal collagen is probably loaded at mid-depths, between the surface and the depth of alveolar collapse. Any subserosal collagen running in series with muscle can be actively recruited over a range of muscle lengths up to the maximum length at alveolar collapse. Coupling subserosal collagen in series with muscle provides an adjustable recruitment, permitting its use over a range of depths when further compression of lung air remains possible. This clearly applies to the array of parallel fibres on the abdominal side. Morphologically, the case is less clear for subserosal collagen on the thoracic side. Although in-series connections with muscle were demonstrable for some of the collagen fibres, it was not for others. It is not conclusive from their structure when or how that collagen is loaded. However, functionally, the premise that subserosal collagen is recruited at mid-depth is strongly supported by the correlation between the thoracic area fraction of subserosal and CCJ collagen and swim speed (Fig. 8B). The correlation accounts for the observed variation in the quantity of subserosal collagen in different species, and it clearly indicates diaphragm loading is affected by some factor associated with locomotion. Such a correlation would not be predicted if subserosal collagen were recruited during respiration or at the point of alveolar collapse.

We therefore conclude cetaceans actively contend with significant P_{di} during a dive. We found the regional distribution of subserosal collagen over the diaphragm reflected the need to withstand or facilitate deformation during a dive, and it was not consistent with loading associated with respiration (prediction 1). Further, recruitment of subserosal collagen could stabilize the diaphragm over a range of dive depths (prediction 2), and fascial collagen, not subserosal collagen, could operate at alveolar collapse (prediction 3). The absence of comparable subserosal collagen on pinniped and sea otter diaphragms is consistent with two interpretations: they experience no significant P_{di} during a dive, or they do experience a P_{di} but diaphragm deformation is not resisted. Consistent with the latter, Falke et al. (2008) have argued that an upwards shift of the diaphragm and an influx of blood into the thorax of Weddell seals compress the lungs more than chest wall compression. In the remaining sections, we evaluate the two possible sources of a P_{di} and then consider the potential consequences of each on the transmural pressures of arteries running in the abdomen.

Fluking and equilibration rate hypotheses

Our findings strongly support the fluking hypothesis. The two specific predictions for the fluking hypothesis were observed: more collagen was found on the cetacean diaphragm than on the pinniped diaphragm, which indicates loading is significant in cetaceans and not significant in pinnipeds and sea otters (Fig. 8A, prediction 4), and the fractional collagen area correlated with cetacean swim performance (Fig. 8B, prediction 5). If this hypothesis proves true, cetaceans experience transient P_{di}

Journal of Experimental Biology (2017) 220, 3464-3477 doi:10.1242/jeb.162289

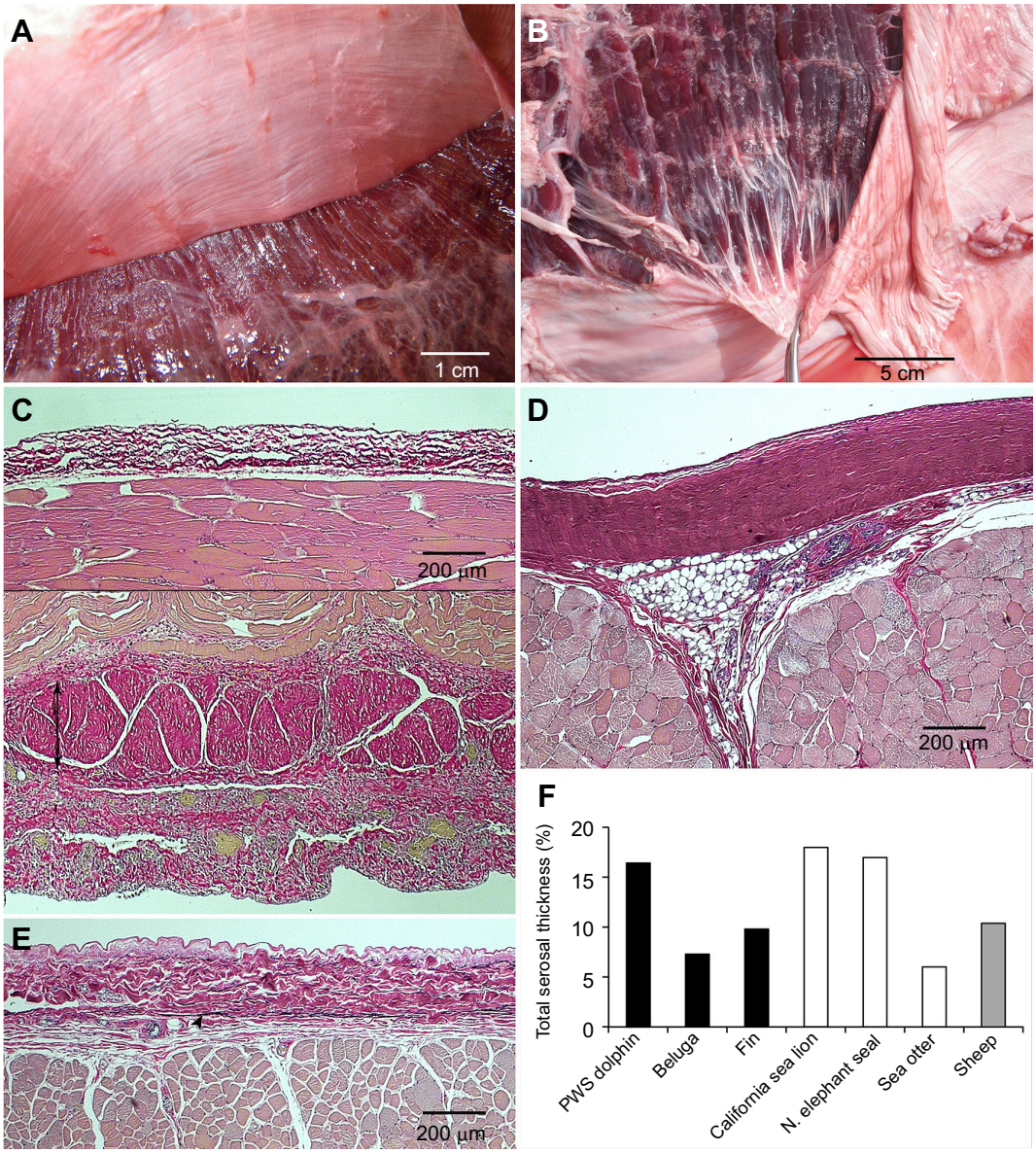

Fig. 9. Pleural and peritoneal fascia in pinniped and cetacean diaphragms. (A) California sea lion, abdominal side. The peritoneum is readily peeled back. Collagen fibres in the serosal fascia run perpendicular to muscle fibres. (B) Fin whale, thoracic side. The pleura is well connected to the underlying costal muscle. Collagen fibres in the serosal fascia run perpendicular to muscle fibres. (C–E) Histological sections cut parallel (C) or perpendicular (D,E) to the muscle fibres. Tissue is stained with Verhoeff's Van Gieson. Fascial collagen fibres run perpendicular to muscle fibres. (C) Crural diaphragm in Pacific white-sided dolphin from a site showing only pleura fascia on the thoracic side (upper panel) and peritoneal fascia and subserosal collagen fibres (double-headed arrow) on the abdominal side (lower panel). (D) Pleural side of costal muscle in California sea lion showing very dense collagen. (E) Peritoneal side of costal muscle in Beluga showing some elastin (arrowhead). (F) Total serosal thickness (pleural plus peritoneal) varied between species, and was similar in cetaceans and non-cetaceans.

on each downstroke, with the magnitude being greater in faster swimmers.

Our results are also consistent with the equilibration rate hypothesis, although the design of this investigation did not allow a strong test of the hypothesis. The fluking and equilibrium rate hypotheses are not mutually exclusive. The equilibration rate hypothesis states the abdomen responds to changing ambient ocean pressures faster than the thorax. Thoracic pressure depends on the deformation of ribs and diaphragm and the volume of venous influx. In theory, a ready response of any one of these three pathways is sufficient to raise thoracic pressure to ambient and so prevent a P_{di} from developing (Brown and Butler, 2000; Scholander, 1940). Therefore, for even a transient P_{di} to develop, both the thoracic body wall and diaphragm must be sufficiently stiff to sustain a sub-ambient thoracic pressure. Pinniped chest walls are highly compliant and appear unable to sustain a sub-ambient pressure (Fahlman et al., 2014; Leith, 1976). Therefore, the observed absence of subserosal collagen on pinniped diaphragms may be secondary to their high chest wall compliance and not locomotor style, as proposed above. Data for cetacean chest wall compliance are limited. Odontocete rib cages appear designed for flexibility (Cotten et al., 2008; Rommel et al., 2006; Rommel and Reynolds, 2009), and many of the caudal cetacean ribs do not attach ventrally to the sternum, giving flexibility between the cranial and caudal ribs (Marx et al., 2016; Slijper, 1962). The chest wall visibly deformed at depth in a diving dolphin (Ridgway et al., 1969) and in simulated

dives of post-mortem specimens (Moore et al., 2011). However, observation suggests the passive cetacean chest wall is stiffer than the pinniped's (Fahlman et al., 2011; Leith, 1976). Additionally, the cetacean chest wall may be actively stabilized to minimize volume and pressure changes during locomotion (Cotten et al., 2008). Given the complexity of the thoracic response, its dependence on abdominal pressures for venous influx and diaphragm movement, and the finite rate at which blood and viscera can flow, it is likely pressures in the thorax and abdomen do not change in parallel during descent and ascent. That is, the equilibration rate hypothesis probably holds.

Implications of pressure differentials for the arterial system

The impact fluking could have on arterial pressures is illustrated in Fig. 1C. The black trace shows a hypothetical transmural pressure wave for an artery within the thorax. Heart rate was set at 50 beats min^{-1} to represent a diving bradycardia (Williams et al., 2015), and intra-arterial pressure was set at the mammalian standard values of 16/10 kPa (120/80 mmHg) above thoracic pressure. We assumed no fluking pressure pulses were transmitted to the thorax. The red line shows the transmural pressure for an artery within the abdomen. Intra-arterial pressure remained at 16/10 kPa, but abdominal pressure outside the artery was varied with a pulse of ±5 kPa relative to thoracic pressure at a fluking frequency of 80 beats min^{-1}. Combining the cardiac and fluking waves in the abdomen created alternating periods of constructive and destructive wave interference. The highest constructive pressure is the sum of the two amplitudes, i.e. 16+5=21 kPa, and the lowest constructive pressure is 10−5=5 kPa. Thus, in this example, fluking broadened the range of arterial transmural pressures from 16/10 kPa in the thorax to 21/5 kPa in the abdomen. The exact shape and range of the combined wave would depend on the amplitude and frequency of fluking and cardiac contraction. Given the complex relationship between heart rate, fluking frequency and depth reported by Williams et al. (2015), abdominal arteries could experience irregular and widely varying transmural pressures. By preventing relief of abdominal pressures, diaphragm stiffening would increase the range of transmural pressures experienced.

Fig. 1D illustrates the possible impact of P_{di} due to unequal equilibration rates on arterial transmural pressures. The black trace is the same as that in Fig. 1C. The postulated slower equilibration of the thorax means its pressures will lag abdominal pressures, leaving thoracic pressure below abdominal pressure on descent, making it harder to maintain transmural pressures. Because of this lag, the arterial transmural pressures are predicted to shift downward, as shown by the blue line. In this case, we set abdominal pressure 12 kPa above thoracic (equivalent to 1.2 m seawater depth). This value is based on a study in which thoracic and abdominal pressures were modelled for a diving fin whale (Lillie et al., 2013). The model predicted pressure differentials of up to 10–20 kPa could develop when diaphragm stretch was prevented. To put this in perspective, maximal tetanic stimulation of the dog diaphragm can generate ∼6 kPa (Hubmayr et al., 1990), and maximal human effort ∼17 kPa (Bellemare and Grassino, 1982; Field et al., 1984). A 12 kPa higher abdominal pressure reduced the blue line to around zero, and any further reduction would push the arteries in the direction of collapse. The red line shows the upward pressure shift, equivalent to hypertension, predicted on ascent if abdominal pressure falls to 12 kPa below thoracic.

The responses illustrated in Fig. 1D are theoretical, and in reality they will be passively moderated by the effects of gravity due to the different body pitch angle on descent and ascent. This includes the separation of internal organs according to tissue density, causing the diaphragm and abdominal viscera to shift downwards (Craig, 1963). It also includes the greater ambient pressure on body parts farther from the surface, causing an animal that spans 10 m of the water column to experience a snout-to-fluke gradient of 101 kPa. Additionally, thoracic pressures can be actively modulated by the diaphragm through the equivalent of a Valsalva or Mueller manoeuvre (expiration or inspiration against a closed mouth). We expect thoracic pressures to be under active control using sensory feedback, but we have no basis to predict the response time. When ambient ocean pressures can increase at 20–30 kPa s^{-1} or faster, active elimination of P_{di} seems unlikely, especially when locomotion is inconsistent. Therefore, a net and probably fluctuating impact of equilibration rate appears unavoidable, and superimposing this on the fluking effects would further broaden the range of transmural pressures experienced by an artery.

We found the morphology of subserosal collagen in cetacean diaphragms is consistent with the hypothesis that cetacean diaphragms do experience significant P_{di} during a dive, and therefore we expect the cetacean vasculature has adapted both to tolerate and also to mitigate the effects of these P_{di} (Slijper, 1962). Lillie et al. (2013) found the diameter of most fin whale arteries changed little with increasing inflation pressure and demonstrated some withstood transmural pressures of up to −50 kPa before collapsing. Therefore, the arterial properties observed in at least one species are consistent with the prediction of widely varying pressures. This has not been examined in other species. The venous systems of both cetaceans and pinnipeds possess many modifications thought to be beneficial for aquatic life (Barnett et al., 1958). A relative lowering of thoracic pressure generally augments venous return, and sphincters around the posterior vena cava in pinnipeds may protect the heart from overload (Harrison and Tomlinson, 1956; Murdaugh et al., 1962). Although functional sphincters have not been documented in cetaceans, we predict they exist and modulate caval flow in the presence of the P_{di}. Muscle that might function as a sphincter has been described for the harbour porpoise (Harrison and Tomlinson, 1956) and bottlenose dolphin (Slijper, 1962) but is thought to be absent in rorquals (Harrison and Tomlinson, 1956; Slijper, 1962). Whether this difference is related to the loading patterns indicated by Fig. 8B needs to be investigated.

Acknowledgements

The authors thank the staff and volunteers of the Vancouver Aquarium and the Vancouver Aquarium's Marine Mammal Rescue Centre, and the Marine Mammal Section, Fisheries and Oceans, Canada, St John's Newfoundland. We thank Kristján Loftsson and the staff at Hvalur hf, Iceland, Daníel Halldórsson at the Marine and Freshwater Research Institute, Reykjavík, Iceland, and Paul Cottrell, Marine Mammal Coordinator, Pacific Region Fisheries and Oceans Canada. We also thank Marina Piscitelli-Doshkov, Kelsey Gil and Alex Werth for their assistance in some of the dissections. We also express our sincere gratitude to John Gosline for his substantial contribution to this project from its inception.

Competing interests

The authors declare no competing or financial interests.

Author contributions

Conceptualization: M.A.L., R.E.S.; Methodology: M.A.L.; Formal analysis: M.A.L.; Investigation: M.A.L., A.W.V., R.E.S.; Resources: S.R., M.H., W.A.M., G.B.S.; Writing - original draft: M.A.L.; Writing - review & editing: M.A.L., A.W.V., S.R., M.H., W.A.M., G.B.S., R.E.S.; Funding acquisition: A.W.V., R.E.S.

Funding

This work was supported by Discovery Grants from the Natural Sciences and Engineering Research Council [RGPIN 312039-13 and RGPAS 446012-13 to

R.E.S. and RGPIN 155397-13 to A.W.V.], and the National Oceanic and Atmospheric Administration [NA10NMF4390250 to W.A.M.]

References

Angelillo, M., Boriek, A. M., Rodarte, J. R. and Wilson, T. A. (2000). Shape of the canine diaphragm. *J. Appl. Physiol.* **89**, 15-20.

Barnett, C. H., Harrison, R. J. and Tomlinson, J. D. W. (1958). Variations in the venous systems of mammals. *Biol. Rev. Camb. Philos. Soc.* **33**, 442-487.

Bellemare, F. and Grassino, A. (1982). Effect of pressure and timing of contraction on human diaphragm fatigue. *J. Appl. Physiol. Respir. Environ. Exerc. Physiol.* **53**, 1190-1195.

Blix, A. S. and Folkow, L. P. (1995). Daily energy expenditure in free living minke whales. *Acta Physiol. Scand.* **153**, 61-66.

Boriek, A. M. and Rodarte, J. R. (1994). Inferences on passive diaphragm mechanics from gross-anatomy. *J. Appl. Physiol.* **77**, 2065-2070.

Boriek, A. M. and Rodarte, J. R. (1997). Effects of transverse fiber stiffness and central tendon on displacement and shape of a simple diaphragm model. *J. Appl. Physiol.* **82**, 1626-1636.

Boriek, A. M., Kelly, N. G., Rodarte, J. R. and Wilson, T. A. (2000). Biaxial constitutive relations for the passive canine diaphragm. *J. Appl. Physiol.* **89**, 2187-2190.

Boriek, A. M., Rodarte, J. R. and Reid, M. B. (2001). Shape and tension distribution of the passive rat diaphragm. *Am. J. Physiol. Regul. Integr. Comp. Physiol.* **280**, R33-R41.

Bramble, D. M. and Carrier, D. R. (1983). Running and breathing in mammals. *Science* **219**, 251-256.

Brown, R. E. and Butler, J. P. (2000). The absolute necessity of chest-wall collapse during diving in breath-hold diving mammals. *Aquat. Mamm.* **26**, 26-32.

Carrier, D. R. (1987). The evolution of locomotor stamina in tetrapods - circumventing a mechanical constraint. *Paleobiology* **13**, 326-341.

Chamberlain, J. S., Metzger, J., Reyes, M., Townsend, D. and Faulkner, J. A. (2007). Dystrophin-deficient mdx mice display a reduced life span and are susceptible to spontaneous rhabdomyosarcoma. *FASEB J.* **21**, 2195-2204.

Cotten, P. B., Piscitelli, M. A., McLellan, W. A., Rommel, S. A., Dearolf, J. L. and Pabst, D. A. (2008). The gross morphology and histochemistry of respiratory muscles in bottlenose dolphins, *Tursiops truncatus*. *J. Morphol.* **269**, 1520-1538.

Craig, A. B. Jr (1963). Heart rate responses to apneic underwater diving and to breath holding in man. *J. Appl. Physiol.* **18**, 854-862.

De Troyer, A. and Wilson, T. A. (2009). Effect of acute inflation on the mechanics of the inspiratory muscles. *J. Appl. Physiol.* **107**, 315-323.

English, A. W. (1976). Limb movements and locomotor function in the California sea lion (*Zalophus californiunus*). *J. Zool.* **178**, 341-364.

Fahlman, A., Loring, S. H., Ferrigno, M., Moore, C., Early, G., Niemeyer, M., Lentell, B., Wenzel, F., Joy, R. and Moore, M. J. (2011). Static inflation and deflation pressure-volume curves from excised lungs of marine mammals. *J. Exp. Biol.* **214**, 3822-3828.

Fahlman, A., Loring, S. H., Johnson, S. P., Haulena, M., Trites, A. W., Fravel, V. A. and Van Bonn, W. G. (2014). Inflation and deflation pressure-volume loops in anesthetized pinnipeds confirms compliant chest and lungs. *Front. Physiol.* **5**, 443.

Falke, K. J., Busch, T., Hoffmann, O., Liggins, G. C., Liggins, J., Mohnhaupt, R., Roberts, J. D., Stanek, K. and Zapol, W. M. (2008). Breathing pattern, CO(2) elimination and the absence of exhaled NO in freely diving Weddell seals. *Respir. Physiol. Neurobiol.* **162**, 85-92.

Farkas, G. A. and Rochester, D. F. (1988). Functional-characteristics of canine costal and crural diaphragm. *J. Appl. Physiol.* **65**, 2253-2260.

Feldkamp, S. D. (1987). Foreflipper propulsion in the California sea lion, zalophus-californianus. *J. Zool.* **212**, 43-57.

Field, S., Sanci, S. and Grassino, A. (1984). Respiratory muscle oxygen consumption estimated by the diaphragm pressure-time index. *J. Appl. Physiol. Respir. Environ. Exerc. Physiol.* **57**, 44-51.

Fish, F. E. (1996). Transitions from drag-based to lift-based propulsion in mammalian swimming. *Am. Zool.* **36**, 628-641.

Fish, F. E. and Rohr, J. J. (1999). Review of dolphin hydrodynamics and swimming performance. Tech. Rep. 1801, Space and Naval Warfare Systems Command, San Diego, CA.

Fish, F. E., Innes, S. and Ronald, K. (1988). Kinematics and estimated thrust production of swimming harp and ringed seals. *J. Exp. Biol.* **137**, 157-173.

Fitz-Clarke, J. R. (2007). Mechanics of airway and alveolar collapse in human breath-hold diving. *Respir. Physiol. Neurobiol.* **159**, 202-210.

Gates, F., McCammond, D., Zingg, W. and Kunov, H. (1980). In vivo stiffness properties of the canine diaphragm muscle. *Med. Biol. Eng. Comput.* **18**, 625-632.

Gosselin, L. E., Martinez, D. A., Vailas, A. C. and Sieck, G. C. (1994). Passive length-force properties of senescent diaphragm: relationship with collagen characteristics. *J. Appl. Physiol.* **76**, 2680-2685.

Griffiths, R. I. and Berger, P. J. (1996). Functional development of the sheep diaphragmatic ligament. *J. Physiol.* **492**, 913-919.

Griffiths, R. I., Shadwick, R. E. and Berger, P. J. (1992). Functional importance of a highly elastic ligament on the mammalian diaphragm. *Proc. R. Soc. Lond. B. Biol. Sci.* **249**, 199-204.

Harrison, R. J. and Tomlinson, J. D. W. (1956). Observations on the venous system in certain pinnipedia and cetacea. *Proc. Zool. Soc. Lond.* **126**, 205-234.

Harrison, R. J., Tomlinson, J. D. and Bernstein, L. (1954). The caval sphincter in Phoca vitulina L. *Nature* **173**, 86-87.

Hubmayr, R. D., Sprung, J. and Nelson, S. (1990). Determinants of transdiaphragmatic pressure in dogs. *J. Appl. Physiol.* **69**, 2050-2056.

Hwang, W., Kelly, N. G. and Boriek, A. M. (2005). Passive mechanics of muscle tendinous junction of canine diaphragm. *J. Appl. Physiol.* **98**, 1328-1333.

Kenyon, K. W. (1969). *The Sea Otter in the Eastern Pacific Ocean: North American Fauna*, Vol. 68. Washington DC: Bureau Sport Fisheries and Wildlife Publ.

Kim, M. J., Druz, W. S., Danon, J., Machnach, W. and Sharp, J. T. (1976). Mechanics of the canine diaphragm. *J. Appl. Physiol.* **41**, 369-382.

Lang, T. G. and Daybell, D. A. (1963). Porpoise performance tests in a seawater tank. *Nav Ord. Test Sta. Tech. Rep.* 3063.

Le Double, A. F. (1897). Diaphragme. In *Traité des Variations du Système Musculaire de l'homme et leur Signification au Point de Vue de l'Anthropologie Zoologique*, vol. **1**, pp. 297-309. Paris: Schleicher Frères publishers.

Lee, H. T. and Banzett, R. B. (1997). Mechanical links between locomotion and breathing: Can you breathe with your legs? *News Physiol. Sci.* **12**, 273-278.

Leith, D. E. (1976). Comparative mammalian respiratory mechanics. *Physiologist* **19**, 485-510.

Lillie, M. A., Piscitelli, M. A., Vogl, A. W., Gosline, J. M. and Shadwick, R. E. (2013). Cardiovascular design in fin whales: high-stiffness arteries protect against adverse pressure gradients at depth. *J. Exp. Biol.* **216**, 2548-2563.

Lockyer, C. and Waters, T. (1986). Weights and anatomical measurements of Northeastern Atlantic Fin (*Balaenoptera-Physalus*, Linnaeus) and Sei (*Balaenoptera-Borealis*, Lesson) whales. *Mar. Mamm. Sci.* **2**, 169-185.

Loring, S. H. and Mead, J. (1982). Action of the diaphragm on the rib cage inferred from a force-balance analysis. *J. Appl. Physiol. Respir. Environ. Exerc. Physiol.* **53**, 756-760.

Mardini, I. A. and Mccarter, R. J. M. (1987). Contractile properties of the shortening rat diaphragm invitro. *J. Appl. Physiol.* **62**, 1111-1116.

Margulies, S. S., Farkas, G. A. and Rodarte, J. R. (1990). Effects of body position and lung volume on in situ operating length of canine diaphragm. *J. Appl. Physiol.* **69**, 1702-1708.

Marx, F. G., Lambert, O. and Uhen, M. D. (2016). *Cetacean Paleobiology*. Chichester: Wiley Blackwell.

McCully, K. K. and Faulkner, J. A. (1983). Length-tension relationship of mammalian diaphragm muscles. *J. Appl. Physiol.* **54**, 1681-1686.

Michailova, T. N. and Usunoff, K. G. (2006). Serosal membranes (Pleura, Pericardium, Peritoneum) - Normal structure, development and experimental pathology. *Adv. Anat. Embryol. Cell Biol.* **183**, 1-142.

Moore, M. J., Hammar, T., Arruda, J., Cramer, S., Dennison, S., Montie, E. and Fahlman, A. (2011). Hyperbaric computed tomographic measurement of lung compression in seals and dolphins. *J. Exp. Biol.* **214**, 2390-2397.

Murdaugh, H. V., Pyron, W. W., Wood, J. W. and Brennan, J. K. (1962). Function of inferior vena cava valve of harbour seal. *Nature* **194**, 700-701.

Pabst, D. A. (1993). Intramuscular morphology and tendon geometry of the epaxial swimming muscles of dolphins. *J. Zool.* **230**, 159-176.

Péan, J. L., Chuong, C. J., Ramanathan, M. and Johnson, R. L. (1991). Regional deformation of the canine diaphragm. *J. Appl. Physiol.* **71**, 1581-1588.

Perry, S. F. and Carrier, D. R. (2006). The coupled evolution of breathing and locomotion as a game of leapfrog. *Physiol. Biochem. Zool.* **79**, 997-999.

Pierce, S. E., Clack, J. A. and Hutchinson, J. R. (2011). Comparative axial morphology in pinnipeds and its correlation with aquatic locomotory behaviour. *J. Anat.* **219**, 502-514.

Piscitelli, M. A., Raverty, S. A., Lillie, M. A. and Shadwick, R. E. (2013). A review of cetacean lung morphology and mechanics. *J. Morphol.* **274**, 1425-1440.

Ridgway, S. H., Scronce, B. L. and Kanwishe, J. (1969). Respiration and deep diving in the bottlenose porpoise. *Science* **166**, 1651-1654.

Road, J., Newman, S., Derenne, J. P. and Grassino, A. (1986). In vivo length-force relationship of canine diaphragm. *J. Appl. Physiol.* **60**, 63-70.

Rommel, S. A. and Reynolds, J. E. (2009). Skeleton, Postcranial. In *Encyclopedia of Marine Mammals* (ed. W. F. Perrin, B. Würsig and J. G. M. Thewissen), pp. 1021-1033. San Diego: Academic Press.

Rommel, S. A., Costidis, A. M., Fernández, A., Jepson, P. D., Pabst, D. A., McLellan, W. A., Houser, D. S., Cranford, T., van Helden, A. L., Allen, D. M. et al. (2006). Elements of beaked whale anatomy and diving physiology and some hypothetical causes of sonar-related stranding. *J. Cetacean Res. Manage.* **7**, 189-209.

Ronald, K., McCarter, R. and Selley, L. J. (1977). Venous circulation in the harp seal (*Pagophilus groenlandicus*). In *Functional Anatomy of Marine Mammals*, Vol. 3 (ed. R. J. Harrison), pp. 235-270. London: Academic Press.

Scholander, P. (1940). Experimental investigations on the respiratory function in diving mammals and birds. *Hvalrådets skrifter* **22**, 1-131.

Slijper, E. J. (1962). *Whales*/*Translated by A. J. Pomerans*. New York: Basic Books.

Strumpf, R. K., Humphrey, J. D. and Yin, F. C. P. (1989). Contributions of muscle and nonmuscle components to biaxial mechanics of passive and tetanized canine diaphragm. In *1989 Advances in Bioengineering* (ed. B. Rubinsky), pp. 203-204. New York: Am. Soc. Mech. Eng.

Strumpf, R. K., Humphrey, J. D. and Yin, F. C. P. (1993). Biaxial mechanical-properties of passive and tetanized canine diaphragm. *Am. J. Physiol.* **265**, H469-H475.

Tarasoff, F. J., Bisaillon, A., Piérard, J. and Whitt, A. P. (1972). Locomotory patterns and external morphology of the river otter, sea otter, and harp seal (Mammalia). *Can. J. Zool.* **50**, 915-929.

Urmey, W. F., De Troyer, A., Kelly, K. B. and Loring, S. H. (1988). Pleural pressure increases during inspiration in the zone of apposition of diaphragm to rib cage. *J. Appl. Physiol.* **65**, 2207-2212.

Williams, T. M. (1989). Swimming by sea otters: adaptations for low energetic cost locomotion. *J. Comp. Physiol. A* **164**, 815-824.

Williams, T. M., Fuiman, L. A., Kendall, T., Berry, P., Richter, B., Noren, S. R., Thometz, N., Shattock, M. J., Farrell, E., Stamper, A. M. et al. (2015). Exercise at depth alters bradycardia and incidence of cardiac anomalies in deep-diving marine mammals. *Nat. Commun.* **6**, 6055.

Williamson, G. R. (1972). The true body shape of rorqual whales. *J. Zool.* **167**, 277-286.

Young, I. S., Alexander, R. M., Woakes, A. J., Butler, P. J. and Anderson, L. (1992). The synchronization of ventilation and locomotion in horses (*Equus-Caballus*). *J. Exp. Biol.* **166**, 19-31.